CRYSTAL GROWTH & DESIGN

Article

pubs.acs.org/crystal

Understanding the *p*-Toluenesulfonamide/Triphenylphosphine Oxide Crystal Chemistry: A New 1:1 Cocrystal and Ternary Phase Diagram

Denise M. Croker,*[,†,§] Michael E. Foreman,[†,‡] Bridget N. Hogan,[†,§] Nuala M. Maguire,[†,‡] Curtis J. Elcoate,[†,‡] Benjamin K. Hodnett,[†,§] Anita R. Maguire,[†,∥] Åke C. Rasmuson,[†,§] and Simon E. Lawrence[†,‡]

[†]Solid State Pharmaceutical Cluster, [‡]Department of Chemistry, Analytical and Biological Chemistry Research Facility, University College Cork, Cork, Ireland

[§]Materials and Surface Science Institute and the Department of Chemical and Environmental Sciences, University of Limerick, Limerick, Ireland

[∥]Department of Chemistry and School of Pharmacy, Analytical and Biological Chemistry Research Facility, University College Cork, Cork, Ireland

Supporting Information

ABSTRACT: A novel 1:1 cocrystal between *p*-toluenesulfonamide and triphenylphosphine oxide has been prepared and structurally characterized. This 1:1 cocrystal was observed to form during solid state grinding experiments, with subsequent formation of a known 3:2 cocrystal in the presence of excess sulfonamide. Both cocrystals are stable in the solid state. The ternary phase diagram for the two coformers was constructed in two different solvents: acetonitrile and dichloromethane. Examination of these diagrams clarified solution crystallization of both the newly discovered 1:1 cocrystal and the previously reported 3:2 cocrystal, and identified regions of stability for each cocrystal in each solvent. The choice of solvent was found to have a significant effect on the position of the solid state regions within a cocrystal system.

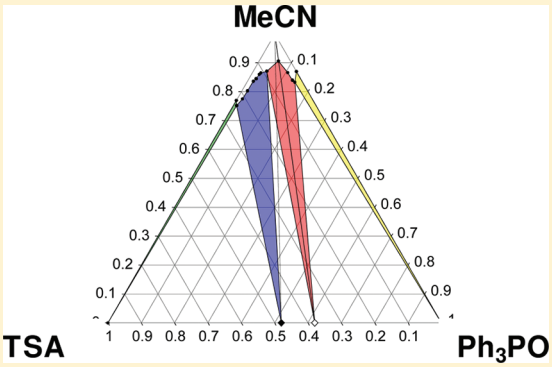

INTRODUCTION

Cocrystals, crystalline structures composed of two or more neutral components, have the potential to alter the physical properties of solid state materials, and as such are of great interest to the pharmaceutical industry.[1] Research in cocrystallization has greatly increased in recent years, yet large scale production of a commercial cocrystal product remains elusive. This is mainly due to a lack of robustness in cocrystal preparation methods. Solid state grinding, solvent drop grinding, and solution methods are routinely used to produce cocrystals,[2,3] but with a certain element of trial and error involved. The majority of the work to date has focused on discovery of new cocrystal structures, although there has been recent work on understanding the mechanism of formation of cocrystals,[4−10] as well as combining prediction and experiment to design novel cocrystal forms.[11]

Ternary phase diagrams can be used to describe the stability of a desired cocrystal in terms of the concentration of both of the coformers in a given solvent.[4−10] Chiarella et al. used ternary phase diagrams to understand the formation of a 1:1 cocrystal of *trans*-cinnamic acid and nicotinamide.[4] Evaporation of a solution containing stoichiometric amounts of both coformers in methanol yielded the cocrystal, but in water gave only the acid. A phase diagram was constructed by allowing the coformers and the cocrystal to equilibrate individually in methanol and water, with varying coformer ratios. In methanol, it was observed that the solubility curve of the cocrystal crossed the 1:1 stoichiometric ratio line, meaning that it is possible to crystallize the cocrystal from a stoichiometic solution in methanol. In water, the cocrystal solubility curve does not cross the 1:1 stoichiometric ratio line, and thus it is not possible to obtain the cocrystal from a stoichiometric aqueous solution. Rodríguez-Hornedo et al. made use of a ternary phase diagram to describe the stability of two cocrystals (2:1 and 1:1 ratios) of carbamazepine with 4-aminobenzoic acid.[7] Both cocrystals could be obtained from slow evaporation of solutions of the coformers in ethanol, with the cocrystal stochiometry dictated by the acid concentration. Billot et al. used discontinuous isoperibolic thermal analysis (DITA) to produce phase diagrams of an active pharmaceut-

Received: September 30, 2011
Revised: December 12, 2011
Published: December 15, 2011

icals ingredient (API) and glutaric acid in a range of different solvents and used the results to build a predictive model for cocrystal stability in alternative solvents.[5] A number of authors have reviewed the thermodynamics involved in cocrystal formation.[9,12−14]

Triphenylphosphine oxide (Ph_3PO) is an excellent hydrogen-bond acceptor and has therefore attracted attention as a cocrystal coformer.[15] Sulfonamides have also been used as coformers due to their hydrogen-bond donor ability, for example, as recently shown by Nangia et al.[16] The commonly observed motif is the R_4^2 (8) ring, usually with a 1:1 stoichiometry. Glidewell et al. reported a 3:2 cocrystal of *p*-toluenesulfonamide (TSA) with Ph_3PO,[17] as well as a 1:1 cocrystal of TSA with the related *m*-tritolylphosphine oxide.[18]

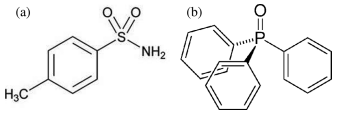

Figure 1. Chemical structure of (a) *p*-toluenesulfonamide (M.P. = 134−137 °C) and (b) triphenylphosphine oxide (M.P. = 154−158 °C).

The cocrystallization of TSA with Ph_3PO was investigated, and herein we report a new 1:1 cocrystal of TSA with Ph_3PO. The formation of the two cocrystals was investigated in the solid state and in solution, and ternary phase diagrams were constructed to identify regions of stability for each cocrystal in two solvents, acetonitrile and dichloromethane.

EXPERIMENTAL SECTION

Chemicals. *p*-Toluenesulfonamide and triphenylphosphine oxide were obtained from Sigma and used as received. Acetonitrile and dichloromethane were reagent grade.

Solid State Grinding Experiments. Grinding experiments were performed using a Retsch MM400 ball mill fitted with 5 mL grinding jars containing one 2.5 mm stainless steel grinding ball per jar. The mill was operated at 30 Hz frequency. The initial experiment involved grinding a 1:1 ratio of the two coformers for 30 min on a 1 mmol scale. Subsequent experiments were undertaken on a 1 mmol as detailed in Tables 1 and 2.

Crystallization Experiments. *p*-Toluenesulfonamide (0.171 g, 1.00 mmol) and triphenylphosphine oxide (0.278 g, 1.00 mmol) were dissolved in MeCN (6 mL) and placed in a sample vial. Toluene (4 mL) was layered on top of the solution, and the system was left to stand for 21 days to give crystals suitable for single crystal diffraction.

p-Toluenesulfonamide (0.171 g, 1.00 mmol) and triphenylphosphine oxide (0.278 g, 1.00 mmol) were dissolved in CH_2Cl_2 (10 mL), placed in a sample vial, and left to stand for 14 days to give crystals suitable for single crystal diffraction.

Large amounts of each cocrystal form were produced by cooling crystallization in a HEL Polyblock — a glass reaction vessel with automated heating and cooling provided by a Julabo UC012T-H Unichiller. For the 3:2 cocrystal, *p*-toluenesulfonamide (2.57 g, 0.015 mmol) and triphenylphosphine oxide (4.17 g, 0.015 mmol) were dissolved in CH_2Cl_2 (50 mL), heated to reflux, and maintained under reflux for 1 h. For the 1:1 cocrystal, *p*-toluenesulfonamide (5.60 g, 0.033 mmol) and triphenylphosphine oxide (11.23 g, 0.040 mmol) were dissolved in MeCN (50 mL), heated to 70 °C, and maintained at this temperature for 1 h. The solutions were cooled at 0.1 ° C min^{-1} to 5 °C, and aged for 24 h. The crystals were isolated, washed with the pure crystallization solvent (~10 mL), and dried in a vacuum oven at 50 °C overnight. Cocrystal form was verified using powder X-ray diffraction (PXRD).

Solubility Measurements. The solubility of pure TSA and Ph_3PO respectively in MeCN and CH_2Cl_2 was determined gravimetrically. Excess solid was charged to solvent at 20 °C and equilibrated with constant agitation for 24 h, at which point agitation was stopped and the solids were allowed to settle for 1 h. Three 1 mL samples of the clear solution were filtered into preweighed glass vials (M_1) and weighed (M_2). The solvent was allowed to evaporate in a fume hood (24 h) before transferring the glass vial to a vacuum oven at 50 ° C (overnight). The vial was allowed to return to room temperature before weighing the final dry weight (M_3). The formula $(M_3 - M_1)/(M_2 - M_3)$ revealed the solubility, expressed as g of solid/g of solvent.

The solubility of pure TSA and the 1:1 cocrystal as a function of Ph_3PO concentration in MeCN and CH_2Cl_2 was determined at 20 °C by equilibrating the desired phase in solutions of known Ph_3PO concentration. The solubility of pure Ph_3PO and the 3:2 cocrystal as a function of TSA concentration in MeCN and CH_2Cl_2 was determined at 20 °C by equilibrating the desired phase in solutions of known TSA concentration. Gravimetric analysis as described above was used to calculate solubility, with mass balance used to account for the mass of the known component.

The solubility of the 1:1 cocrystal in MeCN at 20 ° C was measured in the same way, but efforts to measure the solubility of the 3:2 cocrystal in MeCN, or the 1:1 or 3:2 cocrystal in CH_2Cl_2, were unsuccessful due to transformation of the solid form within the equilibration time.

Invariant points, also referred to as eutectic points or transition concentrations, are fixed solution concentrations at which two solid phases can exist together in equilibrium; in the present work, namely, TSA and the 3:2 cocrystal (C_1), the 3:2 cocrystal and the 1:1 cocrystal (C_2), and the 1:1 cocrystal and Ph_3PO (C_3). These points were determined by generating a slurry of the two required solid forms, described as (C_1), (C_2), (C_3) above, using the method described by Rodríguez-Hornedo et al.[14] The slurries were equilibrated for 24 h at 20 °C, after which the solvent content of the liquid phase was determined using gravimetric analysis, and the concentration of TSA and Ph_3PO in the liquid phase was determined using HPLC.

The experimental setup for all solubility measurements consisted of a thermostatic water bath (Grant GR150 with S38 stainless steel water bath; 26 L; stability ±0.005 °C and uniformity ±0.02 °C @ 37 °C) with a serial magnetic stirrer plate placed on the base. Agitation was provided by use of 10 mm magnetic stirrer bars in 5 mL glass vials.

Construction of the Ternary Phase Diagram. The solubility of the pure substances and the invariant points were converted to mass fraction on a total mass basis (TSA + Ph_3PO + solvent) and plotted on a ternary axis in both MeCN and CH_2Cl_2 to generate the appropriate ternary phase diagrams using ProSim Ternary Diagram software. Mass fraction was chosen in preference to mole fraction as the use of mole fraction tended to compress the solution phase region making visualization of the solubility curves difficult.

Differential Scanning Calorimetry (DSC). DSC was performed on a TA Instruments Q1000 incorporating a refrigerated cooling system. Samples (3−5 mg) were crimped in nonhermetic aluminum pans and scanned from 30 to 300 °C at a heating rate of 10 °C/min under a continuously purged dry nitrogen atmosphere.

Single Crystal Diffraction. X-ray diffraction data were collected on a Bruker APEX II DUO diffractometer using graphite monochromatized Mo Kα radiation (λ = 0.7107 Å) and cooled using an Oxford Cryosystems COBRA fitted with a N_2 generator. All calculations were performed using the *APEX2* software suite,[19,20] and the diagrams were prepared using Mercury 2.4.[21]

Powder Diffraction. Powder diffraction data were collected on either a Philips X'Pert-MPD PRO diffractometer with nickel filtered copper Cu Kα radiation (λ = 1.5418 Å), run at 40 kV and 35 mA, 2θ = 5−35°, with a step size of 0.02° 2θ and a scan speed of 0.02° s^{-1}, or on a Stöe Stadi MP diffractometer with Cu Kα_1 radiation (λ = 1.5406 Å) run at 40 kV and 40 mA, 2θ = 3.5−60°, with a step size of 0.5° 2θ and a step time of 30s.

HPLC Analysis. This was performed on either a Waters Alliance 2690 Separations Module with a Waters 486 Detector using a YMC-Pack ODS-A column (250 mm × 4.6 mm, 5 μm) eluting with MeCN:H_2O (60:40) at 1 mL/min, UV detection at 254 nm, or on a

dx.doi.org/10.1021/cg201300e | Cryst. Growth Des. 2012, 12, 869−875

HPLC System consisting of a Shimadzu LC10AT Pump set at 1.5 mL/min, Shimadzu SPD-6AV Spectrophotometric detector at 254 nm, a Waters 717 autosampler with a Beckman Coulter Ultrasphere ODS Column (250 mm × 4.5 mm, 5 μm), eluting with MeCN:H_2O (60:40).

RESULTS AND DISCUSSION

Solid State Grinding. Solid state grinding of an equimolar mixture of TSA and Ph_3PO for 30 min yielded a product which showed the presence of two sharp endothermic peaks at 135 and 139 °C in the DSC analysis, Figure 2. The 3:2 cocrystal is

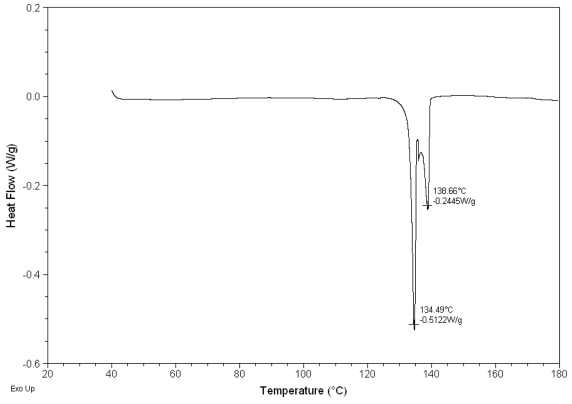

Figure 2. DSC trace of the product obtained from 30 min grinding of a 1:1 molar mixture of TSA and Ph_3PO.

known to have a melting point of 138 °C.[17] The PXRD pattern of this product showed the presence of the known 3:2 cocrystal and extra peaks which were not due to an excess of either starting material.

Single crystal analysis of crystals obtained from MeCN, melting point 134−136 °C, revealed a novel 1:1 cocrystal (Figure 3). Each amide hydrogen atom is involved in a discrete

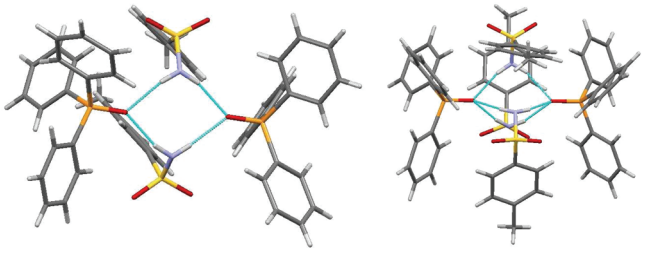

Figure 3. The cocrystals of TSA with PPh_3O: (i) the 1:1 cocrystal, left, showing the R_4^2 (8) ring and (ii) the 3:2 cocrystal,[17] right, which also has the R_4^2 (8) motif.

hydrogen bond to a phosphine oxygen atom, leading to a discrete four molecule hydrogen-bonded complex containing a R_4^2 (8) ring at the binary level.[22] The PXRD data for the unknown material observed in the grinding experiments is consistent with the single crystal data for this new 1:1 cocrystal. Crystals grown from CH_2Cl_2, melting point 138−140 °C, were found to match the reported 3:2 structure.[17] The X-ray diffraction pattern of each form was generated in Mercury 2.4 from the respective crystallographic information files (CIF) file and is presented in Figure 4.

In order to gain some insight into the stability of the cocrystals, we undertook further grinding experiments. Thus, a 1:1 molar ratio of the two coformers was ground for either a short time (5 min) or a long time (198 min). This was repeated using a 3:2 molar ratio of the coformers. The results (Table 1) suggest that the 1:1 cocrystal is formed first, before transforming into the 3:2 cocrystal if sufficient sulfonamide is present.

Examination of the crystal structures of the 1:1 and 3:2 cocrystals show significant similarity: they both possess two terminal PPh_3O molecules, with sulfonamide molecules acting as bridges via hydrogen bonding. This suggests that a third sulfonamide can "slot into" the structure of the 1:1 cocrystal in the grinding experiments to generate the 3:2 cocrystal.

To test this hypothesis, the following experiments were undertaken: (i) the 1:1 cocrystal was ground with TSA in a 1:1 ratio, (ii) the 1:1 cocrystal (1 equiv) was ground with TSA (2 equiv), and (iii) the 3:2 cocrystal was ground with Ph_3PO in a 1:1 ratio (Table 2 and Supporting Information). Experiments (i) and (ii) confirm that the 1:1 cocrystal can transform to the 3:2 cocrystal with excess sulfonamide present. Experiment (iii) shows that the 3:2 cocrystal does not transform to the 1:1 cocrystal when ground with an excess of Ph_3PO. PXRD analysis indicates no changes to either cocrystal over the period of 18 months. Having examined the stability of the cocrystals in the solid state, we proceeded to undertake solution-based stability studies.

Solubility Measurements. The solubility values for TSA and Ph_3PO in each solvent at 20 °C are listed in Table 3. The order of solubility between TSA and Ph_3PO varies in the two solvents: TSA is more soluble than Ph_3PO in MeCN, but much less soluble than Ph_3PO in CH_2Cl_2. Ph_3PO is extremely soluble in CH_2Cl_2, exceeding the solubility of TSA by a factor of 35. It has been reported that the relative solubilities of the two cocrystal components in a solvent can be used to prepare a cocrystal in that solvent,[4] and a screening method has been developed around this concept.[23]

Production of pure cocrystal forms using cooling crystallization was confirmed using PXRD (Figure 4). The solubility of the 1:1 cocrystal was successfully determined in MeCN. The concentration of TSA in a solution in equilibrium with the 1:1 cocrystal is lower than the concentration of TSA in a solution in equilibrium with pure TSA. The solubility of the 3:2 cocrystal could not be determined in MeCN. Equilibration of the 3:2 cocrystal in MeCN resulted in formation of the 1:1 cocrystal within 24 h, a phenomenon known as incongruent dissolution.

Both cocrystals dissolved incongruently in CH_2Cl_2. Equilibration of the 3:2 cocrystal resulted in the formation of pure TSA, and equilibration of the 1:1 cocrystal resulted in the production of a mixture of the 3:2 cocrystal and TSA. Incongruent dissolution is an indication of an unsymmetrical ternary phase diagram and usually occurs when there is a large difference in solubility between the two pure conforming phases in that solvent.[4]

Experimentally determined invariant points in each solvent are expressed in terms of mass fraction in Table 4.

The ternary phase diagrams in MeCN and CH_2Cl_2 are presented in Figures 5 and 6 respectively.

TSA and Ph_3PO have a reasonably similar solubility in MeCN resulting in an approximately symmetrical ternary phase diagram. The 3:2 (region 4) and 1:1 (region 6) cocrystal are independently stable across a wide range of solution compositions. The 1:1 component stoichiometric line (solid line) intersects the solubility curve for the 1:1 cocrystal, indicating congruent dissolution for this cocrystal. Dissolution of the 1:1 cocrystal results in a solution with 1:1 molar

dx.doi.org/10.1021/cg201300e | Cryst. Growth Des. 2012, 12, 869−875

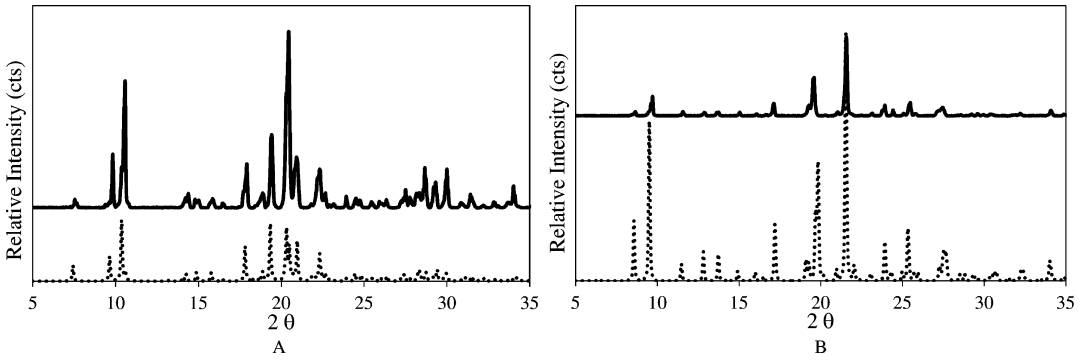

Figure 4. PXRD patterns recorded for the 1:1 (A) and 3:2 (B) cocrystals of TSA and Ph_3PO. Experimental patterns are shown as solid lines with the corresponding theoretical pattern given as a dotted line.

Table 1. Effect of Reagent Composition and Grinding Time upon Cocrystal Output

material input	grind time (min)	material output
1:1 ratio of coformers	5	1:1 cocrystal, plus both coformers
1:1 ratio of coformers	198	1:1 cocrystal
3:2 ratio of coformers	5	1:1 cocrystal, plus both coformers
3:2 ratio of coformers	198	3:2 cocrystal

Table 2. Effect of Grinding the Cocrystal with One Coformer

material input	grind time (min)	material output
1:1 cocrystal with TSA (1:1 ratio)	20	3:2 cocrystal plus TSA
1:1 cocrystal with TSA (2:1 ratio)	20	3:2 cocrystal
3:2 cocrystal with Ph_3PO (1:1 ratio)	20	3:2 cocrystal plus Ph_3PO

Table 3. Measured Solubility Values for each Solid Form in MeCN and CH_2Cl_2 at 20 °C, Expressed in Terms of Mass Fraction (Total Mass Basis, (MF)), and Molarity [M]

		solubility				
solid	solvent	MF_{TSA}	MF_{Ph_3PO}	$MF_{solvent}$	[M]	solid phase at end of equilibration
TSA	MeCN	0.23		0.77	1.38	TSA
Ph_3PO			0.13	0.87	0.40	Ph_3PO
1:1 cocrystal		0.04	0.06	0.90	0.19	1:1
3:2 cocrystal			N/A			1:1
TSA	CH_2Cl_2	0.01		0.99	0.11	TSA
Ph_3PO			0.44	0.56	3.80	Ph_3PO
1:1 cocrystal			N/A			3:2 + TSA
3:2 cocrystal			N/A			TSA

stoichiometry, making it possible to experimentally measure the solubility of the 1:1 cocrystal in MeCN. In contrast, the 3:2 component stoichiometric line (dashed line) does not intersect the solubility curve of the 3:2 cocrystal, explaining the observed incongruent dissolution of this form. This line instead intersects the solubility curve for the 1:1 cocrystal. Dissolution of the 3:2 cocrystal results in establishment of an equilibrium between a saturated solution and the 1:1 cocrystal.

Table 4. Invariant Points in MeCN and CH_2Cl_2 at 20 °C

		invariant point (mass fraction, total mass basis)		
solvent	solid forms in equilibrium	X_{TSA}	X_{Ph_3PO}	$X_{Solvent}$
MeCN	TSA + 3:2 (C_1)	0.195	0.014	0.791
	3:2 + 1:1(C_2)	0.087	0.041	0.871
	1:1 + Ph_3PO (C_3)	0.018	0.150	0.832
CH_2Cl_2	TSA + 3:2 (C_1)	0.047	0.075	0.878
	3:2 + 1:1 (C_2)	0.035	0.205	0.760
	1:1 + Ph_3PO (C_3)	0.031	0.357	0.612

In CH_2Cl_2 the significant difference in solubility between TSA and Ph_3PO results in an unsymmetrical diagram, with all regions skewed toward the Ph_3PO axis of the diagram. Both cocrystals dissolve incongruently, with dissolution of the 3:2 cocrystal initially resulting in solution of invariant composition in equilibrium with the 3:2 cocrystal and pure TSA (region 3), potentially continuing to a solution in equilibrium with pure TSA (region 2). Dissolution of the 1:1 cocrystal initially results in generation of a solution saturated with respect to the 1:1 and the 3:2 cocrystal (region 5), with continued dissolution resulting in solution composition moving to region 4, the region of stability for the 3:2 cocrystal. The 1:1 component stoichiometric line will eventually pass through the C_1 invariant point on this diagram, resulting in a saturated solution of invariant composition in equilibrium with the 3:2 cocrystal and pure TSA. In each case, the extent of dissolution will be controlled by the mass of the solvent present. The diagram is in good agreement with the phase conversions observed during efforts to measure cocrystal solubility (Table 3).

Evaporation from a solution of 1:1 molar composition in either solvent may be visualized by following the solid line from the top apex of the diagram to the 1:1 cocrystal composition point. In MeCN, this line passes straight through region 6 making it possible to isolate the 1:1 cocrystal from this solution, regardless of the point at which evaporation is stopped. In CH_2Cl_2, evaporation of a solution of 1:1 molar composition could initially result in crystallization of pure TSA as the solid line skims the solubility curve for TSA. Continued evaporation will move the solution composition into region 4, making it possible to isolate a pure 3:2 cocrystal product, but only if evaporation is stopped within this region. Further evaporation will result in concomitant crystallization of the 1:1 cocrystal as the solution composition moves into region 5. This demonstrates that the product of an evaporative crystallization can be dependent on the extent of solvent evaporation in a

dx.doi.org/10.1021/cg201300e | Cryst. Growth Des. 2012, 12, 869–875

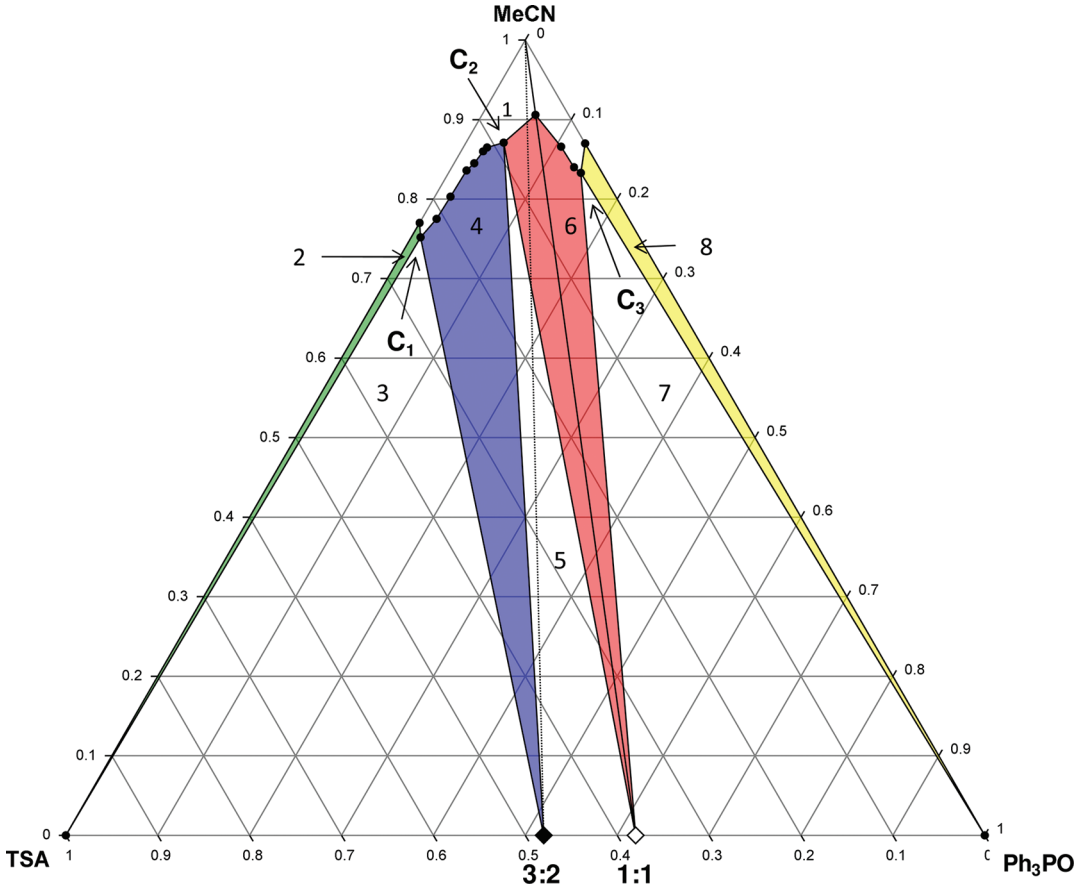

Figure 5. Ternary phase diagram for the TSA–Ph_3PO–MeCN system at 20 °C. Regions in the diagram are as follows: (1) solution phase; all other regions consist of a saturated solution in contact with (2) TSA only, (3) TSA + 3:2 cocrystal, (4) 3:2 cocrystal only, (5) 3:2 cocrystal + 1:1 cocrystal, (6) 1:1 cocrystal only, (7) 1:1 cocrystal + Ph_3PO, and (8) Ph_3PO only. Values are in mass fractions.

cocrystallization experiment, depending on the shape of the ternary phase diagram. A ternary phase diagram represents a system at thermodynamic equilibrium, and the above discussion is based on the assumption that thermodynamic equilibrium is maintained during the evaporation process. Crystallization is a dynamic process in which kinetic and thermodynamic factors compete to determine the solid product form, with kinetic factors most likely to promote the formation of a metastable product, but this is not specifically addressed in this work.

The same seven solid form regions (regions 2–8) were observed in each solvent, but the choice of solvent did affect the positioning of each solid form region within the ternary phase diagram. The shape of a ternary phase diagram is dependent on the relative solubility of both coformers in that solvent. Selection of a solvent which has a particular affinity for either, or both, coformers is a means of controlling the shape of the ternary phase diagram, and the region of stability for the desired crystal form.

■ CONCLUSIONS

A novel 1:1 cocrystal of *p*-toluenesulfonamide and triphenylphosphine oxide has been obtained by crystallizing the two coformers from acetonitrile, and single crystal analysis successfully applied to identify the new crystal structure. The 1:1 cocrystal has some structural similarity to the known 3:2 cocrystal, with the latter related by a simple incorporation of an extra sulfonamide molecule between two bridging phosphine oxide molecules.

Construction of the ternary phase diagram for *p*-toluenesulfonamide and triphenylphosphine oxide in MeCN and CH_2Cl_2 clearly identified regions of stability for the 1:1 and 3:2 cocrystal in these solvents, allowing for rationalization of the experimental isolation of the 1:1 cocrystal from a solution of 1:1 molar stoichiometry in MeCN, and the 3:2 cocrystal from a solution of 1:1 molar stoichiometry in CH_2Cl_2. This result demonstrates that solution stoichiometry during cocrystal preparation or screening does not necessarily reflect the stoichiometry of the resulting cocrystal. The solubility of both cocrystal coformers must be taken into consideration when performing a cocrystal search to ensure that cocrystals are discovered and that those of different stoichiometry are not missed.

Congruent and incongruent cocrystal dissolution was observed in MeCN for the 1:1 and the 3:2 cocrystal, respectively, with both cocrystals dissolving incongruently in CH_2Cl_2. Incongruent dissolution prevents the measurement of pure cocrystal solubility with traditional methods, as it becomes impossible to equilibrate the pure cocrystal in the pure solvent to generate the required saturated solution. Incongruent dissolution is likely when there is a significant difference between the solubility of the pure coformers in the solvent.

Knowledge of the ternary phase diagram informs effective experimental design to control the desired cocrystal form. The choice of solvent in a cocrystal system has a major impact on the shape of the resulting ternary phase diagram.

dx.doi.org/10.1021/cg201300e | *Cryst. Growth Des.* 2012, 12, 869–875

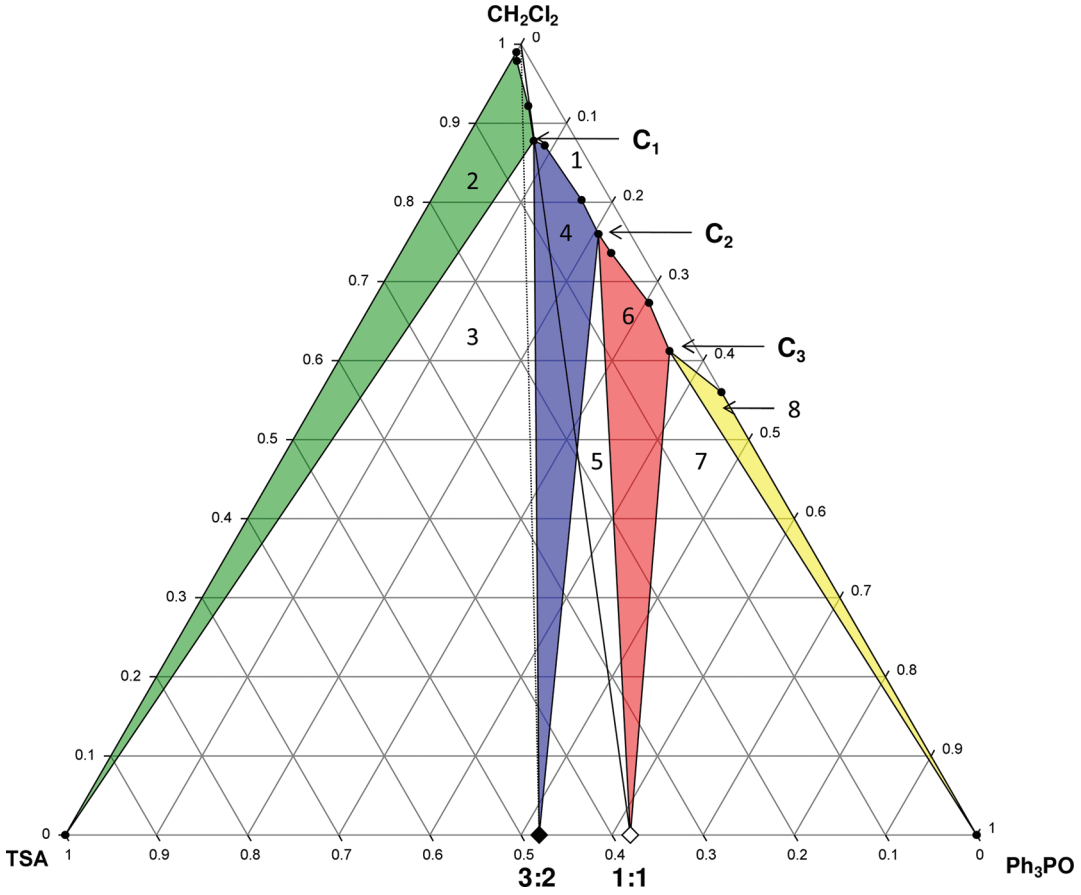

Figure 6. Ternary phase diagram for the TSA−Ph_3PO−CH_2Cl_2 system at 20 °C. Regions in the diagram are as follows: (1) solution phase; all other regions consist of a saturated solution in contact with (2) TSA only, (3) TSA + 3:2 cocrystal, (4) 3:2 cocrystal only, (5) 3:2 cocrystal + 1:1 cocrystal, (6) 1:1 cocrystal only, (7) 1:1 cocrystal + Ph_3PO, and, (8) Ph_3PO only. Values are in mass fraction, total mass basis.

■ ASSOCIATED CONTENT

Supporting Information

X-ray crystallographic information in CIF format, DSC and PXRD data, and additional figures. This material is available free of charge via the Internet at http://pubs.acs.org. The crystallographic data for the 1:1 cocrystal have been deposited with the Cambridge Crystallographic Data Centre, CCDC number 843627. These data can be obtained free of charge from The Cambridge Crystallographic Data Centre via www.ccdc.cam.ac.uk/data_request/cif.

■ AUTHOR INFORMATION

Corresponding Author

*E-mail: Denise.Croker@ul.ie. Tel.: +353 61 234617. Fax: +353 61 213529.

■ ACKNOWLEDGMENTS

This publication has emanated from research conducted with the financial support of Science Foundation Ireland under Grant Numbers 07/SRC/B1158 and 05/PICA/B802/EC07.

■ REFERENCES

(1) Schultheiss, N.; Newman, A. *Cryst. Growth Des.* **2009**, *9*, 2950−2967.
(2) Trask, A. V.; Jones, W. *Top. Curr. Chem.* **2005**, *254*, 41−70.
(3) (a) Weyna, D. R.; Shattock, T.; Vishweshwar, P.; Zaworotko, M. J. *Cryst. Growth Des.* **2009**, *9*, 1106−1123. (b) Trask, A. V.; Motherwell, W. D. S.; Jones, W. *Chem. Commun.* **2004**, 890−891.
(4) Chiarella, R. A.; Davey, R. J.; Peterson, M. L. *Cryst. Growth Des.* **2007**, *7*, 1223−1226.
(5) Ainouz, A.; Authelin, J.-R.; Billot, P.; Liebermann, H. *Int. J. Pharm.* **2009**, *374*, 82−89.
(6) Chadwick, K.; Davey, R. J.; Sadiq, G.; Cross, W.; Pritchard, R. *CrystEngComm* **2009**, *11*, 412−414.
(7) Jayasankar, A.; Reddy, L. S.; Bethune, S. J.; Rodriguez-Hornedo, N. *Cryst. Growth Des.* **2009**, *9*, 889−897.
(8) Yu, Z. Q.; Chow, P. S.; Tan, R. B. H. *Cryst. Growth Des.* **2010**, *10*, 2382−2387.
(9) Nehm, S. J.; Rodríguez-Sprong, B.; Rodríguez-Hornedo, N. *Cryst. Growth Des.* **2006**, *6*, 592−600.
(10) Chadwick, K.; Davey, R. J.; Dent, G.; Pritchard, R. G.; Hunter, C. A.; Musumeci, D. *Cryst. Growth Des.* **2009**, *9*, 1990−1999.
(11) Arlin, J.-B.; Price, L. S.; Price, S. L.; Florence, A. J. *Chem. Commun.* **2011**, *47*, 7074−7076.
(12) Schartmann, R. *Int. J. Pharm.* **2009**, *365*, 77−80.
(13) Good, D. J.; Rodríguez-Hornedo, N. *Cryst. Growth Des.* **2010**, *10*, 1028−1032.
(14) Good, D. J.; Rodríguez-Hornedo, N. *Cryst. Growth Des.* **2009**, *9* (5), 2252−2264.
(15) (a) Etter, M. C.; Baures, P. W. *J. Am. Chem. Soc.* **1988**, *110*, 639−40. (b) Aakeröy, C. B.; Salmon, D. J. *CrystEngComm* **2005**, *7*, 439−448.
(16) Goud, N. R.; Babu, N. J.; Nangia, A. *Cryst. Growth Des.* **2011**, *11*, 1930−1939.
(17) Ferguson, G.; Glidewell, C. *J. Chem. Soc., Perkin Trans.* **1988**, *II*, 2129−2132.
(18) Ferguson, G.; Lough, A. J.; Glidewell, C. *J. Chem. Soc., Perkin Trans.* **1989**, *II*, 2065−2070.
(19) *APEX2 v2009.3-0*; Bruker AXS: Madison, WI, 2009.

(20) Sheldrick, G. M. *Acta Crystallogr., Sect. A* **2008**, *64*, 112−122.
(21) Macrae, C. F.; Bruno, I. J.; Chisholm, J. A.; Edgington, P. R.; McCabe, P.; Pidcock, E.; Rodríguez-Monge, L.; Taylor, R.; van de Streek, J.; Wood, P. A. *J. Appl. Crystallogr.* **2008**, *41*, 466−470.
(22) Etter, M. C. *Acc. Chem. Res.* **1990**, *23*, 120−126.
(23) Ter Horst, J. H.; Deji, M. A.; Cains, P. W. *Cryst. Growth Des.* **2009**, *9* (3), 1531−1537.